Supporting Information

Sustainable and Energy–Efficient Production of Rare–Earth Metals via Chloride-based Molten Salt Electrolysis

Authors:
Benjamin Holcombe[1,4,=], Nicholas Sinclair[1,4,=], Ruwani Wasalathanthri[1,4], Badri Mainali[1,4], Evan Guarr[1], Alexander A. Baker[2,4], Sunday Oluwadamilola Usman[3,4], Eunjeong Kim[2,4], Shohini Sen-Britain,[2,4] Hongyue Jin[3,4], Scott K. McCall[2,4], Rohan Akolkar[1,4,#]

Affiliations:
[1]Department of Chemical Engineering, Case Western Reserve University, Cleveland OH 44106
[2]Materials Science Division, Lawrence Livermore National Laboratory, Livermore CA 94550
[3]Systems and Industrial Engineering, University of Arizona, Tucson, AZ 85721
[4]Critical Materials Institute, Ames, IA 50011

Table of Contents

1. Chlorination of Neodymium Ore

Neodymium chloride ($NdCl_3$) used as raw material for electrowinning of Nd in our process can be obtained by controlled chlorination of neodymium oxide upon treatment with HCl (reaction S1). The standard free energy change for this neutralization reaction is a negative value indicating that the reaction is thermodynamically favored and a stable $NdCl_3$ is readily and non-carbothermically obtained. Also, H_2O obtained as a byproduct can be reacted with Cl_2 (byproduct of electrolysis of $NdCl_3$) forming HCl, which can then be circulated back to the system making the overall process a closed loop. Figure S1 shows feasibility of chlorination of Nd_2O_3.

$$Nd_2O_3 + 6HCl \rightarrow 2NdCl_{3(aq)} + 3H_2O_{(l)} \qquad \Delta G^0 = -141 \text{ kJ} \qquad [S1]$$

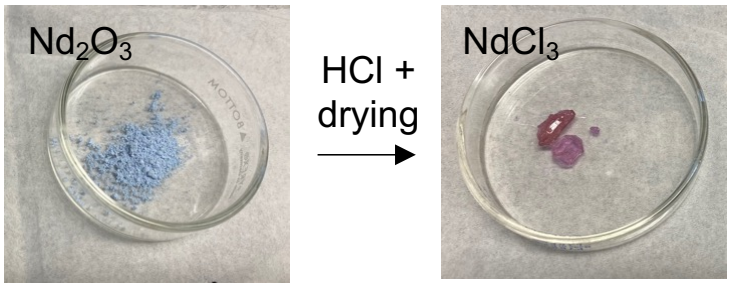

Figure S1: Chlorination of Nd_2O_3 by treatment with dilute HCl forming $NdCl_3$ along with H_2O as a by-product. Bluish white powder of Nd_2O_3 (as received) was treated with stoichiometric amount of 0.1 M $HCl_{(aq)}$. Upon stirring, Nd_2O_3 was completely neutralized by HCl. The aqueous reaction product obtained thereby was then subjected to drying by exposure to open atmosphere resulting in pinkish $NdCl_3$ crystals.

2. Cathode Analysis: Reproducibility, Production of Dense Deposit, Effect of Water

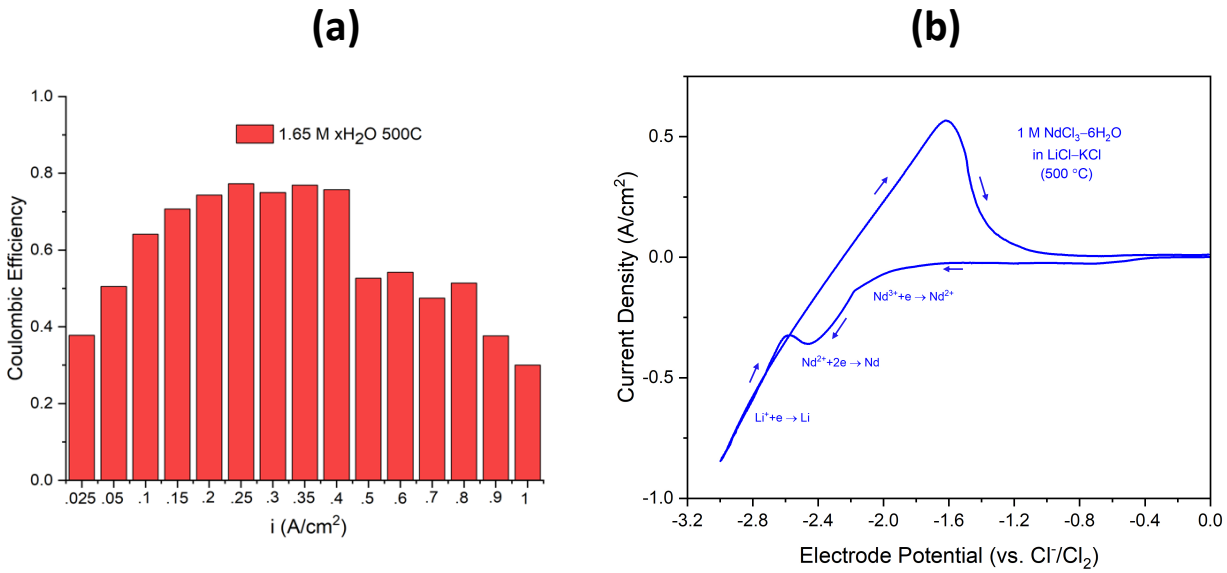

Figure S2: Coulombic efficiency (a) as a function of plating current density when performing chloride MSE using a hydrated $NdCl_3$ salt. In the 200–400 mA/cm^2 current density range, efficiency approaches 80% at 500 ºC. Cyclic voltammetry (b) displays no observable major peak associated with the reduction of water when starting from $NdCl_3$ hydrate salts. The Nd deposition reaction is followed by Li deposition at more negative potentials, as expected at current densities above 500 mA/cm^2.[1]

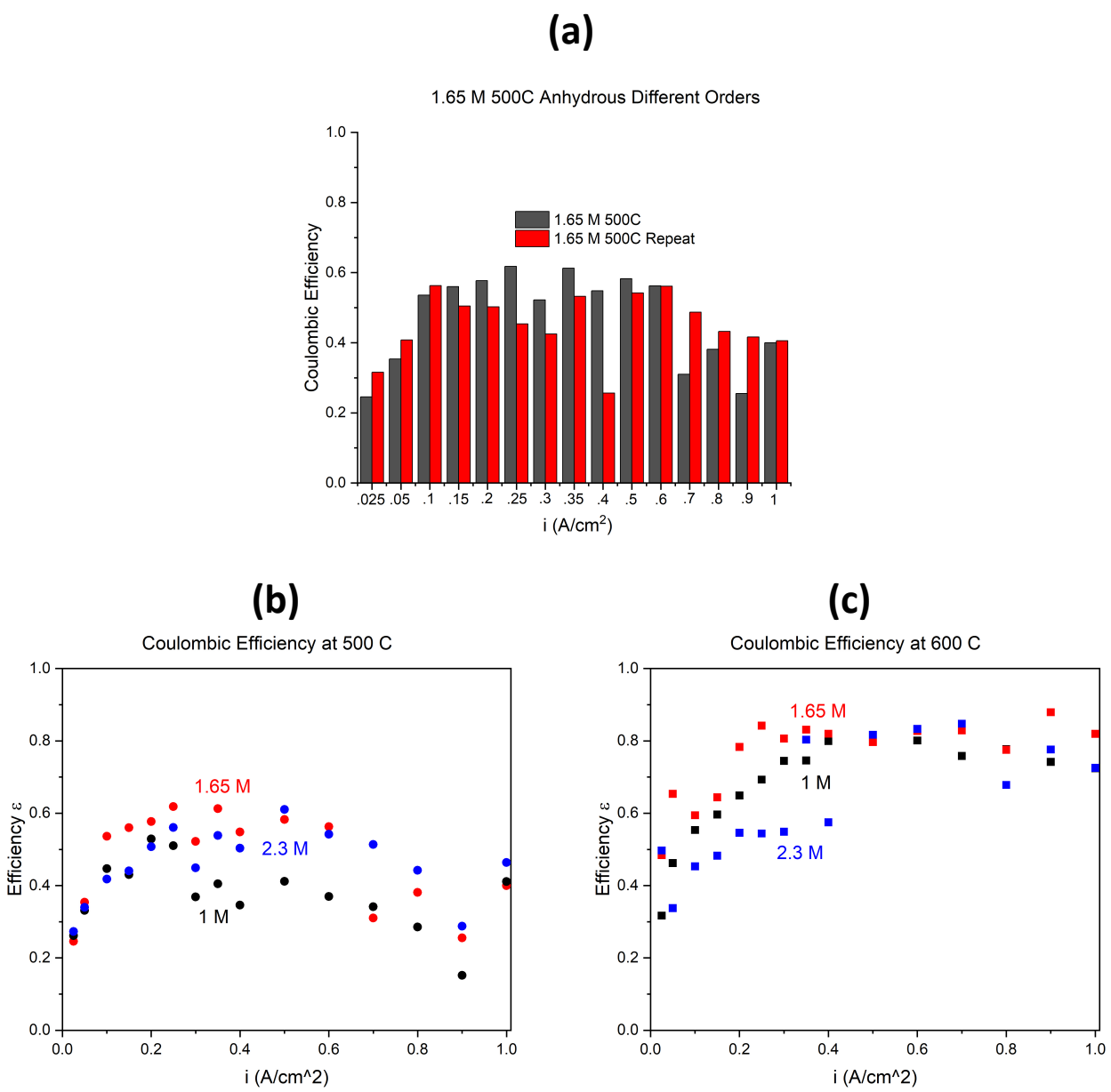

Figure S3: Coulombic efficiency as a function of plating current density when performing chloride MSE using anhydrous $NdCl_3$ salt. Panel (a) shows the general reproducibility of observed trends while in panel (b) it can be seen that at 500 C there is not a distinguishable trend in efficiency as a function of concentration of $NdCl_3$. However, in panel (c), we can see that increasing temperature to 600 C increases efficiency (compared to 500 C) for all concentrations.

When employing hydrated $NdCl_3$, a concern during electrowinning is the co-production of hydrogen via electrolysis of H_2O. However, we have shown using plating/stripping coulometry, that the Nd electrowinning efficiency is maintained at high levels, e.g., ~80% at current densities in the 200–400 mA/cm^2 range (Fig. S2). This combined with no observable water reduction peak in the voltammetry,

suggests that the H_2O is likely evaporated at high temperatures during chloride MSE, or if it is retained in the molten salt, H_2O does not negatively impact performance. Chloride MSE, depending on operating conditions can produce powder, sponge, or dense deposit. Our work has demonstrated conditions that, even when starting from hydrated neodymium salts, can produce compact metallic deposits with minimal salt inclusion. One such dense deposit from hydrated salt can be seen in Fig. S4. This deposit was produced on a W cathode subjected to 0.5 A/cm^2 current density in a 1.65 M $NdCl_3.6H_2O$ containing LiCl–KCl melt at 500 ºC for 1 hour.

Figure S4: Dense neodymium deposit produced with chloride MSE. This deposit was produced on a W cathode subjected to 0.5 A/cm^2 current density in a 1.65 M $NdCl_3.6H_2O$ containing LiCl–KCl melt at 500 ºC for 1 hour. This shows feasibility of utilizing hydrated $NdCl_3$ as the feedstock.

To understand changes to the Nd composition in the electrolyte after electrolysis, UV-Vis was performed at room temperature on samples of the corresponding electrolyte dissolved in 0.1 M HCl using an Agilent Cary 3500 UV-VIS Spectrometer. One gram each of solid electrolyte from before heating and electrolysis and after heating to 500 C, electrolysis for 1 hour and subsequent cooling to room temperature was dissolved into a total volume of 5 mL of 0.1 M HCl in DI. Spectrometry from 750-450 nm is shown in Fig. S5. This range of wavelengths has been reported to contain characteristic Nd peaks in LiCl-KCL melts.[2] A small reduction in the Nd associated peaks can be seen after electrolysis due to the some $NdCl_3$ being consumed during plating.

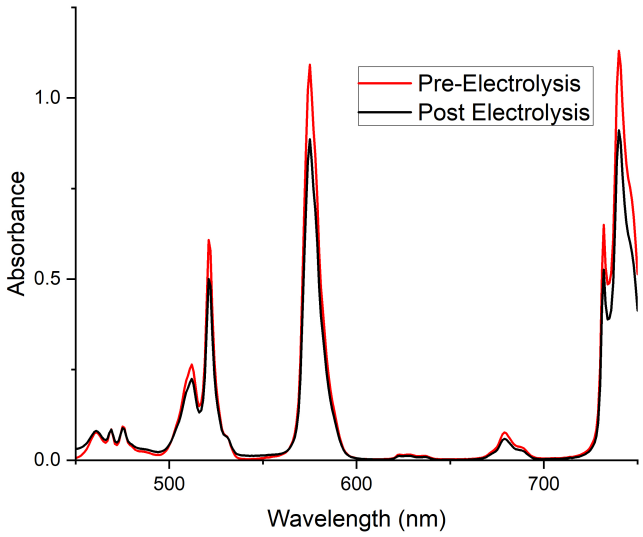

Figure S5. UV-vis spectrometry of the MSE electrolyte components dissolved in 0.1 M HCl before and after 1 hr of MSE operation. The small decrease in peak intensity is likely due to $NdCl_3$ consumption due to electrolysis.

3. Anode Stability

Mass spectrometry of the atmosphere sampled directly above a cell during electrolysis was performed using a Dycor LCD 300 Residual Gas Analyzer (RGA). It was found that chlorine partial pressure above the cell (Fig. S6) rapidly increased after the start of electrolysis, directly correlated with changes in current during the experiment and returned to atmospheric baseline after current was stopped. This shows that chlorine is indeed generated during electrolysis. Future work is planned to construct a divided cell in which the head space around each electrode can be individually swept and the composition of any gases generated at each electrode can be more carefully characterized under a variety of operating conditions.

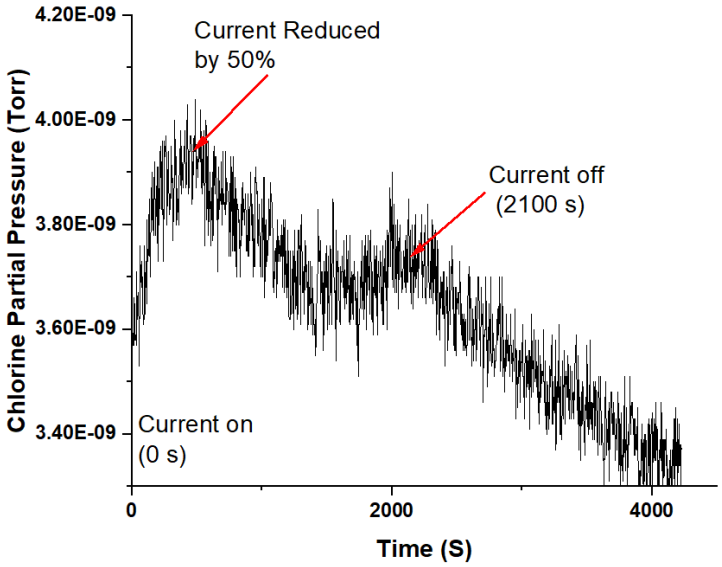

Figure S6. Chlorine partial pressure (mass 35, as measured using an RGA) above a cell operated in atmosphere increases over the atmospheric baseline when current is passed and trends with the magnitude of the current. When current is stopped the partial pressure of mass 35 returns to atmospheric baseline.

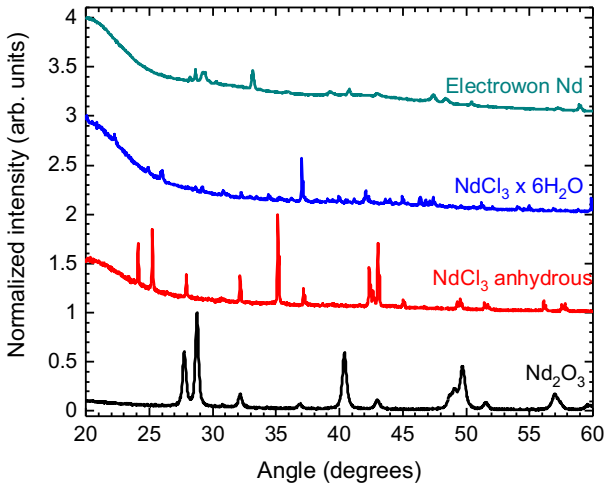

Figure S7. X-ray diffraction (XRD) of Nd_2O_3, Neodymium chloride ($NdCl_3$), $NdCl_3 \cdot 6H_2O$ and Nd produced using chloride MSE. The presence of trapped salts in the Nd deposit complicates the XRD analysis somewhat, but some conclusions can be drawn. None of the strong $NdCl_3$ or $NdCl_3.6H_2O$ peaks are observed in the Nd spectrum, suggesting successful removal of the chlorine during the MSE process. There is evidence of Nd_2O_3 formation, again likely due to surface oxidation during handling (samples were prepared in a glovebox and XRD was run using Bruker inert sample holders, but some leakage is inevitable). The remaining peaks can be indexed to Nd metal, and to KCl, LiCl from the electrolyte salts. The results confirm Nd product formation during electrolysis, similar to the FIB/SEM analysis reported in manuscript.

The evolution of the Ru coating on the DSAs was assessed using time of flight secondary ion mass spectrometry (TOF-SIMS). Anodes were depth profiled before and after operation, ion intensity as a function of sputter time is plotted in Fig. S8. The pre-operation figure shows clear evidence of Ru, giving way to C as the layer is sputtered. The post-operation anode displays the same Ru signature, though it decays much more quickly, indicating a thinner layer in this sample. Further, significant Li and Nd ions are present as remnants of the electrolyte and product that remain despite sonicating in de-ionized water. These results confirm that the Ru survives operation of the anode, but its presence may be rather diminished. Whether this is by leaching of the coating layer, or through mechanical exfoliation, or is simply an artifact of the depth profiling in the presence of salt impurities is unclear. Optimization of coating adhesion and survivability will be the subject of future research.

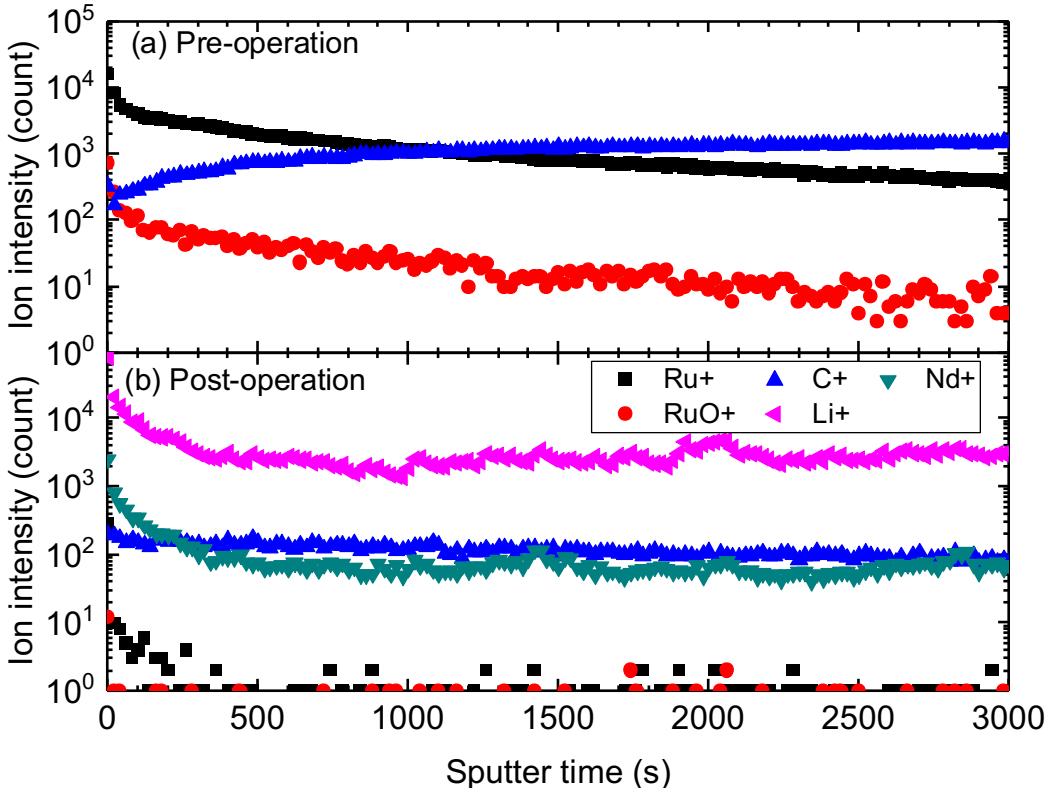

Figure S8. Evolution of the Ru coating on the DSAs was assessed using time of flight secondary ion mass spectrometry (TOF-SIMS). The TOF-SIMS results show that the relative proportion of Ru decreases after 1 hr operation, possibly as a result of some leaching or mechanical exfoliation. Nevertheless, Ru is present on the surface after the operation of the anodes, so some Ru does survive MSE and remains adhered to the anode samples. The depth profiling offered by this data remains inexact, as we were unable to calibrate sputter time to a measured depth, and differing sputter yields means that the two data sets cannot be precisely compared. Nevertheless, there is evidence that the anodes do survive the process with some surface evolution and contamination by salt.

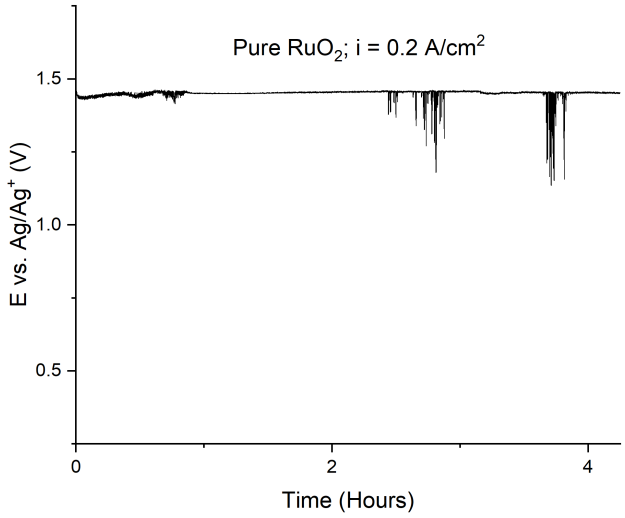

Figure S9: Anode (RuO_2) overpotential was measured with respect to a Ag/Ag^+ reference electrode during chloride MSE at 200 mA/cm^2 at 500 ºC. The anode potential is stable over the duration of galvanostatic electrolysis (4 hours). Also, the total overpotential is (1.45–1.1) = 0.35 V most of which is the ohmic (IR) drop between the anode and the reference probe (estimated IR is 0.29 V). This once again confirms the catalytic nature of the RuO_2 anode, which provides an activation overpotential for Cl_2 evolution of about 60 mV at 200 mA/cm^2.

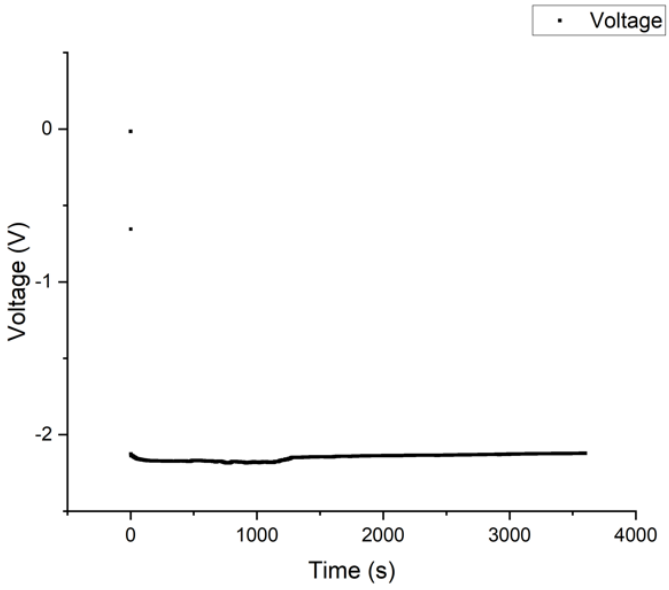

Figure S10: Cathode overpotential during Nd deposition on a Mo sheet was measured with respect to a Ag/Ag^+ reference electrode during chloride MSE at 200 mA/cm^2 at 500 ºC. Cathode overpotential is stable over 1 hour of electrolysis, but the slight depolarization may be due to surface area evolution on account of the deposit roughness.

4. Life Cycle Assessment (LCA)

DSA-based MSE excluding Nd oxides, contribution analysis showed that electricity had a major impact on global warming (see Supporting Information Table S2). Electricity was also the environmental hotspot for conventional MSE process, excluding Nd oxide (see Supporting Information Table S3 – S6). This result indicates the importance of finding a more sustainable energy source for both MSE processes. DSA-based MSE benefits from no graphite consumption and no direct emissions (e.g., CO_2), and this advantage is shown in Table S1 and the subsequent LCA results in Table S2.

Table S1: LCI of DSA-based chloride MSE and conventional MSE for producing 1 kg of Nd metal [a) Emission into air; w) Emission into water].

	Unit	This Study	Arshi et al., (2018)	Lee and Wen (best) (2018)	Lee and Wen (average) (2018)	Lee and Wen (worst) (2018)	Unit Process
Inputs							
Electricity	kWh	7.33E+00	8.38E+00	9.50E+00	1.03E+01	1.10E+01	Electricity, medium voltage {US}| market group for | A
Graphite	kg		1.86E-01	2.50E-01	2.60E-01	2.70E-01	Graphite {GLO}| market for | APOS, U
Lithium fluoride	kg		8.00E-03	1.00E-02	1.25E-02	1.50E-02	Lithium fluoride {GLO}| market for | APOS, U
Lithium chloride	kg	6.56E-02					Lithium chloride {GLO}| market for | APOS, U
Potassium chloride	kg	8.02E-02					Potassium chloride, as K2O {GLO}| market for | APOS, U
Molybdenum	kg		2.50E-04				Molybdenum {GLO}| market for | APOS, U
Neodymium oxide	kg	1.17E+00	1.17E+00	1.15E+00	1.20E+00	1.25E+00	(Arshi et al., 2018)
Ruthenium oxide	kg	1.73E-05					Estimated from Ruthenium {GLO} | primary productio processing | production mix, at plant | 12.37 g/cm3 |
Neodymium fluoride	kg		8.00E-02	1.40E-01	1.45E-01	1.50E-01	(Arshi et al., 2018)
Hydrochloric acid	kg	7.58E-01					Hydrochloric acid, without water, in 30% solution state for | APOS, U

Steel, unalloyed	kg		3.00E-03				Steel, unalloyed {GLO}| market for | APOS, U
Water, deionized	kg	4.29E+01	4.29E+01	8.00E+00	8.00E+00	8.00E+00	Water, deionized, from tap water, at user {GLO}| mark U
Refractory	kg		2.75E-02				Refractory, fireclay, packed {GLO}| market for | APOS, U
Sodium hydroxide, 50%	kg		2.50E-04				Sodium hydroxide, without water, in 50% solution state market for | APOS, U
Quicklime	kg		2.50E-03				Quicklime, milled, packed {GLO}| market for | APOS, U
Calcium hydroxide	kg			1.65E-01	1.79E-01		Lime, hydrated, packed {GLO}| market for | APOS, U
Emissions							
Calcium fluoride	kg			7.40E-02	7.60E-02		
CO_2	kg		1.11E-01	2.94E-01	3.07E-01	3.20E-01	
CO	kg		3.36E-01				
Hydrogen fluoride	kg			1.75E-04	6.25E-04	4.57E-02	
Fluoride[w)]	kg		2.00E-04	8.00E-05	8.00E-05	8.00E-05	
Particulates, <2.5 μm	kg		1.00E-05				
Particulates, 2.5–10 μm	kg		2.30E-03				

Suspended solids[w)]	kg	5.60E-04	1.60E-03	1.60E-03
Unspecified oils[w)]	kg	4.00E-05	4.00E-05	4.00E-05
Chemical oxygen demand	kg	6.40E-04	6.40E-04	6.40E-04
Total phosphorous[w)]	kg	2.40E-05	2.40E-05	2.40E-05
Total nitrogen[w)]	kg	4.00E-04	4.00E-04	4.00E-04
Ammonia[w)]	kg	2.00E-04	2.00E-04	2.00E-04
Total zinc[w)]	kg	1.20E-05	1.20E-05	1.20E-05
Thorium[w)]	kg	8.00E-07	8.00E-07	8.00E-07
Cadmium[w)]	kg	6.40E-07	6.40E-07	6.40E-07
Lead[w)]	kg	4.00E-06	4.00E-06	4.00E-06
Arsenic[w)]	kg	2.40E-06	2.40E-06	2.40E-06
Chromium[w)]	kg	8.00E-06	8.00E-06	8.00E-06
Chromium (VI)[w)]	kg	2.40E-06	2.40E-06	2.40E-06
Particulate dust	kg	1.50E-03	1.50E-03	1.50E-03
Chloride[a)]	kg	1.25E-03	1.25E-03	1.25E-03

Hydrochloric acid[a)]	kg	2.00E-03	2.00E-03	2.00E-03
Nitrous oxide[a)]	kg	5.00E-03	5.00E-03	5.00E-03
Thorium[a)]	kg	3.00E-06	3.00E-06	3.00E-06

Table S2: LCA results for producing 1 kg of Nd by DSA-based chloride MSE as proposed here.

Impact category	Unit	Total	Lithium chloride	Potassium chloride	Ruthenium oxide	Nd oxide	Electricity	Hydrochloric acid	Water
Ozone depletion	kg CFC-11 eq	2.13E-05	3.83E-08	5.56E-09	9.67E-12	2.07E-05	2.43E-07	3.08E-07	5.09E-09
Global warming	kg CO2 eq	1.36E+02	2.47E-01	3.58E-02	2.63E-01	1.31E+02	3.92E+00	4.37E-01	2.51E-02
Smog	kg O3 eq	2.19E+01	1.95E-02	2.63E-03	2.60E-02	2.17E+01	1.10E-01	3.80E-02	1.33E-03
Acidification	kg SO2 eq	1.09E+00	1.41E-03	1.48E-04	2.98E-03	1.08E+00	1.07E-02	3.04E-03	1.16E-04
Eutrophication	kg N eq	2.44E-01	2.08E-03	1.14E-04	4.85E-05	2.14E-01	2.52E-02	2.67E-03	9.73E-05
Carcinogenics	CTUh	1.25E-08	1.63E-11	4.00E-12	4.81E-12	4.69E-09	1.63E-10	4.75E-11	7.58E-09
Non carcinogenics	CTUh	2.07E-07	5.88E-10	1.27E-10	2.75E-12	1.88E-07	5.73E-09	1.48E-09	1.12E-08
Respiratory effects	kg PM2.5 eq	3.23E-01	2.62E-04	2.30E-05	3.35E-04	3.13E-01	9.01E-03	4.11E-04	3.33E-05
Ecotoxicity	CTUe	1.06E+02	2.70E-01	5.13E-02	1.57E-03	1.02E+02	3.55E+00	6.68E-01	2.74E-01
Fossil fuel depletion	MJ surplus	2.27E+02	2.34E-01	7.32E-02	5.56E-02	2.22E+02	3.62E+00	6.07E-01	1.83E-02

Table S3: LCA results for producing 1kg of Nd by conventional MSE (Arshi et al. 2018)

Impact category	Unit	Total	Neodymium Fluoride	Nd oxide	Electricity	Direct emission	Graphite	Lithium fluoride	Molybdenum	Steel	Wate
Ozone depletion	kg CFC-11 eq	2.15E-05	5.08E-07	2.07E-05	2.78E-07	0.00E+00	1.74E-09	3.95E-09	2.10E-10	2.91E-10	5.09E-
Global warming	kg CO2 eq	1.41E+02	4.27E+00	1.32E+02	4.48E+00	1.11E-01	1.27E-02	4.27E-02	4.14E-03	5.47E-03	2.51E-
Smog	kg O3 eq	2.23E+01	3.20E-01	2.18E+01	1.26E-01	1.87E-02	1.71E-03	3.27E-03	1.21E-03	3.02E-04	1.33E-
Acidification	kg SO2 eq	1.12E+00	3.04E-02	1.08E+00	1.23E-02	0.00E+00	8.79E-05	8.25E-04	6.33E-05	1.80E-05	1.16E-
Eutrophication	kg N eq	4.55E-01	2.11E-01	2.15E-01	2.88E-02	0.00E+00	3.25E-05	5.00E-04	2.55E-04	1.82E-05	9.73E-
Carcinogenics	CTUh	1.28E-08	2.79E-10	4.71E-09	1.87E-10	0.00E+00	2.30E-12	2.76E-12	6.40E-13	4.63E-13	7.58E-
Non carcinogenics	CTUh	2.17E-07	9.48E-09	1.89E-07	6.55E-09	0.00E+00	3.02E-11	1.01E-10	6.06E-10	2.21E-10	1.12E-
Respiratory effects	kg PM2.5 eq	3.29E-01	4.16E-03	3.14E-01	1.03E-02	6.53E-04	1.67E-05	4.44E-05	2.29E-05	6.64E-06	3.33E-
Ecotoxicity	CTUe	1.15E+02	8.46E+00	1.02E+02	4.05E+00	0.00E+00	1.43E-02	4.36E-02	3.30E-02	1.28E-01	2.74E-
Fossil fuel depletion	MJ surplus	2.31E+02	3.82E+00	2.23E+02	4.13E+00	0.00E+00	1.72E-02	5.54E-02	3.18E-03	2.43E-03	1.83E-

Table S4: LCA results for producing 1 kg of Nd by conventional MSE (Lee and Wen, best-case scenario, 2018)

Impact category	Unit	Total	Neodymium fluoride	Nd oxide	Electricity	Emissions	Graphite	Lithium fluoride	Water	Calcium hydroxide
Ozone depletion	kg CFC-11 eq	2.16E-05	8.90E-07	2.04E-05	3.15E-07	0.00E+00	2.33E-09	4.93E-09	9.50E-10	1.15E-08
Global warming	kg CO2 eq	1.44E+02	7.47E+00	1.29E+02	5.08E+00	1.78E+00	1.70E-02	5.34E-02	4.67E-03	1.59E-01
Smog	kg O3 eq	2.21E+01	5.60E-01	2.14E+01	1.43E-01	0.00E+00	2.31E-03	4.09E-03	2.49E-04	3.78E-03
Acidification	kg SO2 eq	1.13E+00	5.31E-02	1.06E+00	1.39E-02	2.04E-03	1.18E-04	1.03E-03	2.15E-05	2.29E-04
Eutrophication	kg N eq	6.14E-01	3.69E-01	2.11E-01	3.27E-02	1.56E-04	4.36E-05	6.25E-04	1.81E-05	9.27E-05
Carcinogenics	CTUh	3.22E-08	4.89E-10	4.63E-09	2.11E-10	2.54E-08	3.09E-12	3.45E-12	1.41E-09	7.22E-12

Non carcinogenics	CTUh	2.12E-07	1.66E-08	1.86E-07	7.43E-09	5.76E-11	4.06E-11	1.26E-10	2.10E-09	9.37E-11
Respiratory effects	kg PM2.5 eq	3.28E-01	7.27E-03	3.09E-01	1.17E-02	0.00E+00	2.24E-05	5.55E-05	6.21E-06	3.30E-05
Ecotoxicity	CTUe	1.20E+02	1.48E+01	1.00E+02	4.59E+00	2.52E-01	1.92E-02	5.45E-02	5.11E-02	4.57E-02
Fossil fuel depletion	MJ surplus	2.31E+02	6.68E+00	2.19E+02	4.69E+00	0.00E+00	2.31E-02	6.92E-02	3.42E-03	1.05E-01

Table S5: LCA results for producing 1 kg of Nd by conventional MSE (Lee and Wen, average-case scenario, 2018)

Impact category	Unit	Total	Neodymium fluoride	Nd oxide	Electricity	Emissions	Graphite	Lithium fluoride	Water	Calcium hydroxide
Ozone depletion	kg CFC-11 eq	2.25E-05	9.21E-07	2.13E-05	3.42E-07	0.00E+00	2.43E-09	6.17E-09	9.50E-10	1.25E-08
Global warming	kg CO2 eq	1.50E+02	7.74E+00	1.35E+02	5.51E+00	1.80E+00	1.77E-02	6.68E-02	4.67E-03	1.72E-01
Smog	kg O3 eq	2.31E+01	5.80E-01	2.23E+01	1.55E-01	0.00E+00	2.40E-03	5.11E-03	2.49E-04	4.10E-03
Acidification	kg SO2 eq	1.18E+00	5.50E-02	1.11E+00	1.51E-02	2.76E-03	1.23E-04	1.29E-03	2.15E-05	2.49E-04
Eutrophication	kg N eq	6.39E-01	3.82E-01	2.20E-01	3.55E-02	1.56E-04	4.54E-05	7.81E-04	1.81E-05	1.01E-04
Carcinogenics	CTUh	3.24E-08	5.06E-10	4.83E-09	2.29E-10	2.54E-08	3.21E-12	4.31E-12	1.41E-09	7.83E-12
Non carcinogenics	CTUh	2.21E-07	1.72E-08	1.94E-07	8.05E-09	5.76E-11	4.22E-11	1.58E-10	2.10E-09	1.02E-10
Respiratory effects	kg PM2.5 eq	3.42E-01	7.53E-03	3.22E-01	1.27E-02	0.00E+00	2.33E-05	6.94E-05	6.21E-06	3.58E-05
Ecotoxicity	CTUe	1.25E+02	1.53E+01	1.04E+02	4.98E+00	2.52E-01	2.00E-02	6.81E-02	5.11E-02	4.96E-02
Fossil fuel depletion	MJ surplus	2.41E+02	6.92E+00	2.29E+02	5.08E+00	0.00E+00	2.40E-02	8.65E-02	3.42E-03	1.14E-01

Table S6: LCA results for producing 1 kg of Nd by conventional MSE (Lee and Wen, worst-case scenario, 2018)

Impact Category	Unit	Total	Neodymium fluoride	Nd oxide	Electricity	Emissions	Graphite	Lithium fluoride	Water
Ozone depletion	kg CFC-11 eq	2.35E-05	9.53E-07	2.21E-05	3.65E-07	0.00E+00	2.52E-09	7.40E-09	9.50E-10
Global warming	kg CO2 eq	1.56E+02	8.00E+00	1.41E+02	5.88E+00	1.81E+00	1.84E-02	8.01E-02	4.67E-03
Smog	kg O3 eq	2.40E+01	6.00E-01	2.33E+01	1.66E-01	0.00E+00	2.49E-03	6.13E-03	2.49E-04
Acidification	kg SO2 eq	1.30E+00	5.69E-02	1.15E+00	1.61E-02	7.49E-02	1.28E-04	1.55E-03	2.15E-05
Eutrophication	kg N eq	6.64E-01	3.96E-01	2.29E-01	3.79E-02	1.56E-04	4.71E-05	9.37E-04	1.81E-05
Carcinogenics	CTUh	3.27E-08	5.24E-10	5.03E-09	2.45E-10	2.54E-08	3.33E-12	5.17E-12	1.41E-09
Non carcinogenics	CTUh	2.31E-07	1.78E-08	2.02E-07	8.60E-09	5.76E-11	4.38E-11	1.89E-10	2.10E-09
Respiratory effects	kg PM2.5 eq	3.57E-01	7.79E-03	3.35E-01	1.35E-02	0.00E+00	2.42E-05	8.33E-05	6.21E-06
Ecotoxicity	CTUe	1.30E+02	1.59E+01	1.09E+02	5.32E+00	2.52E-01	2.07E-02	8.18E-02	5.11E-02
Fossil fuel depletion	MJ surplus	2.51E+02	7.16E+00	2.38E+02	5.43E+00	0.00E+00	2.50E-02	1.04E-01	3.42E-03

Table S7: Sensitivity analysis for global warming potential (GWP in kg of CO_2 equivalent) from producing 1 kg of Nd metal, using DSA-based chloride MSE. For example, if Nd oxide to Nd metal conversion efficiency is 100% and ruthenium oxide coating is used for 10 hours before recoating, then the GWP is 162 kg of CO_2 equivalent for producing 1 kg of Nd metal.

RuO_2 coating reuse time (hrs)	**GWP (kg of CO_2 equivalent)**
10	162
100	139
500	137
1000	**136**
1500	**136**
2000	**136**

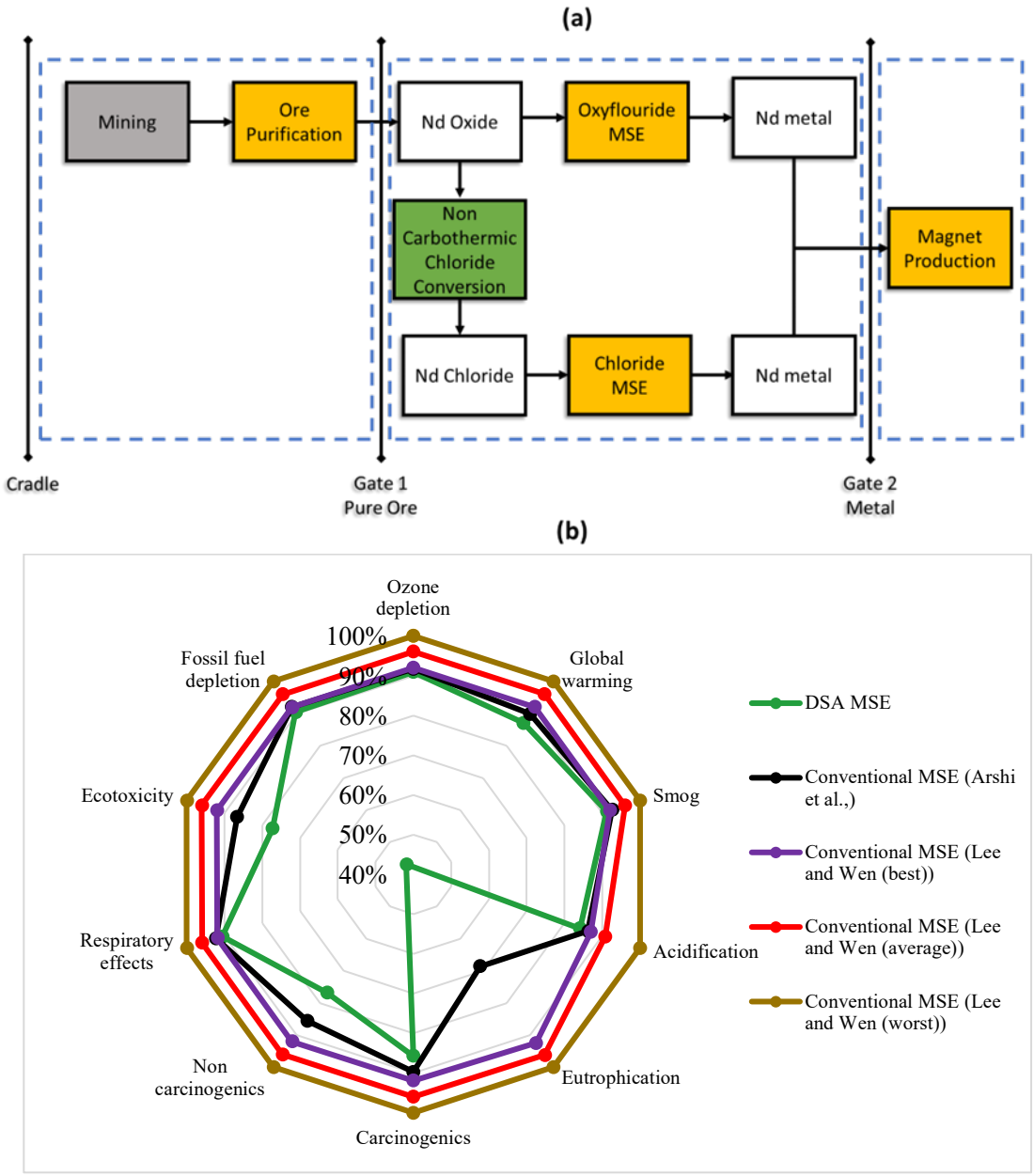

Figure S11. A partial schematic of the life cycle of a NdFeB magnet (a) outlines the various gates that can be used to define the bounds considered during LCA. Cradle-to-Gate 2 LCA (b) including all steps from neodymium mining to neodymium metal production.

SI References

1. Wang, Y.; Liu, Q.; Quan, M.; Liu, Y.; Chen, Y.; Ren, P.; Zhang, Z.; Liu, Y. Efficient Recovery of the Fission Element Neodymium by Electrodeposition from Molten LiCl–KCl and Research on the Thermodynamics and Dynamics of Processes. ACS Sustainable Chemistry & Engineering 2022, 10 (38), 12796-12807. DOI: 10.1021/acssuschemeng.2c03712.
2. Hayashi, H. Akabori, M. Ogawa, T. and Minato, K. "Spectrophotometric Study of Nd^{2+} Ions in LiCl-KCl Eutectic Melt." Zeitschrift Naturforschung Teil A (2004) 59, 705-710.